

1
2
3
4 1 ***De Novo* PacBio long-read and phased avian genome assemblies correct and**
5 **add to reference genes generated with intermediate and short reads**
6 2
7 3

8
9 4 Jonas Korlach^{1*}, Gregory Gedman², Sarah B. Kingan¹, Chen-Shan Chin¹, Jason T.
10 5 Howard², Jean-Nicolas Audet^{2,3}, Lindsey Cantin², and Erich D. Jarvis^{2,4*}
11 6

12
13 7 ¹Pacific Biosciences, Menlo Park, CA 94025, USA; ²Laboratory of Neurogenetics of Language,
14 8 The Rockefeller University, New York, NY 10065, USA; ³Department of Biology, McGill
15 9 University, Montreal, Quebec H3A 1B1, Canada; ⁴Howard Hughes Medical Institute, Chevy
16 10 Chase, MD 20815, USA
17 11

18
19
20 12 *Corresponding authors: jkorlach@pacb.com and ejarvis@rockefeller.edu
21 13

22
23 14 Jonas Korlach, Ph.D.
24 15 Chief Scientific Officer
25 16 Pacific Biosciences
26 17 1305 O'Brien Drive
27 18 Menlo Park, CA 94025
28 19 650-521-8006
29 20

30
31
32 21 Erich D. Jarvis, Ph.D.
33 22 Investigator, Howard Hughes Medical Institute
34 23 Professor, The Rockefeller University, Box 54
35 24 1230 York Avenue, New York, New York 10065
36 25 212 327-8806
37 26
38 27
39 28
40
41
42
43
44
45
46
47
48
49
50
51
52
53
54
55
56
57
58
59
60
61
62
63
64
65

1
2
3
4
5
6
7
8
9
10
11
12
13
14
15
16
17
18
19
20
21
22
23
24
25
26
27
28
29
30
31
32
33
34
35
36
37
38
39
40
41
42
43
44
45
46
47
48
49
50
51
52
53
54
55
56
57
58
59
60
61
62
63
64
65

29 Abstract

30
31 **Background:** Reference quality genomes are expected to provide a resource for studying gene
32 structure, function, and evolution. However, often genes of interest are not completely or
33 accurately assembled, leading to unknown errors in analyses or additional cloning efforts for the
34 correct sequences. A promising solution is long-read sequencing. Here we tested PacBio-based
35 long-read sequencing and diploid assembly for potential improvements to the Sanger-based
36 intermediate-read zebra finch reference and Illumina-based short-read Anna’s hummingbird
37 reference, two vocal learning avian species widely studied in neuroscience and genomics.

38 **Results:** With DNA of the same individuals used to generate the reference genomes, we
39 generated diploid assemblies with the FALCON-Unzip assembler, resulting in contigs with no
40 gaps in the megabase range, representing 150-fold and 200-fold improvements over the current
41 zebra finch and hummingbird references, respectively. These long-read assemblies corrected and
42 resolved what we discovered to be numerous misassemblies in the references, including missing
43 sequences in gaps, erroneous sequences flanking gaps, base call errors in difficult to sequence
44 regions, complex repeat structure errors, and allelic differences between the two haplotypes.
45 These corrections were validated by single long genome and transcriptome reads, and resulted
46 for the first time in completely resolved protein-coding genes widely studied in neuroscience and
47 specialized in vocal learning species.

48 **Conclusions:** These findings demonstrate the impact of long reads and phasing haplotypes on
49 generating high quality assemblies necessary for understanding gene structure, function, and
50 evolution.

51
52 **Keywords:** De novo genome assembly, long reads, SMRT Sequencing, brain, language.

55 Background

56
57 Having available genomes of species of interest provides a powerful resource to rapidly conduct
58 investigations on genes of interest. For example, using the costly Sanger method to sequence
59 genomes of the two most commonly studied bird species, the chicken [1] and zebra finch [2],
60 have impacted many studies. The zebra finch is a vocal learning songbird, with the rare ability to
61 imitate sounds as humans do for speech; comparative analyses of genes in its genome has
62 allowed insights into the mechanisms and evolution of spoken-language in humans [2-4]. With
63 the advent of more cost-effective next generation sequencing technologies using short reads, 10-
64 fold more genomes were sequenced, with one large successful project being the Avian
65 Phylogenomics Consortium, which generated genomes of 45 new bird species across the family
tree and several reptiles [5]. The consortium was successful in conducting comparative genomics
and phylogenetics with populations of genes [6-9]. However, when it was necessary to dig
deeper into individual genes, it was discovered that many were incompletely assembled or

1
2
3
4 69 contained apparent misassemblies. For example, the *DRD4* dopamine receptor was missing in
5 70 half of the assemblies, in part due to sequence complexity [10]. The *EGR1* immediate early gene
6 71 transcription factor, a commonly studied gene in neuroscience and in vocal learning species, was
7 72 missing the promoter region in an GC-rich region in every bird genome we examined. Another
8 73 immediate early gene, *DUSP1*, with specialized vocalizing-driven gene expression in song nuclei
9 74 of vocal learning species, has microsatellite sequences in the promoters of vocal learning species
10 75 that are missing or misassembled, requiring single-molecule cloning and sequencing to resolve
11 76 [11]. Such errors create a great amount of effort to clone, sequence, and correct assemblies of
12 77 individual genes of interest.

13
14 78 High-throughput, single-molecule, long-read sequencing shows promise to alleviate these
15 79 problems [12-14]. Here, we applied PacBio single-molecule long-read (1,000-60,000 bp)
16 80 sequencing and diploid assembly on two vocal learning species, the zebra finch previously
17 81 assembled with Sanger-based intermediate reads (700-1,000 bp), and the Anna's hummingbird
18 82 previously assembled with Illumina-based short reads (100-150 bp). We found that the long-read
19 83 diploid assemblies resulted in major improvements in genome completeness and contiguity, and
20 84 completely resolved the problems in all of our genes of interest. This study is part of an effort to
21 85 help evaluate standards for the G10K vertebrate (<https://genome10k.soe.ucsc.edu>) and the B10K
22 86 bird (<http://b10k.genomics.cn/index.html>) genome consortiums.
23 87
24 88

25 89 **Results**

26 90 **The long-read assemblies result in 150-fold to 200-fold increases in contiguity**

27 91 To generate long-read assemblies, high molecular weight DNA was isolated from muscle tissue
28 92 of the same zebra finch male and Anna's hummingbird female used to create the current
29 93 reference genomes [2, 6]. The DNA was sheared, 35-40 kb libraries generated, size-selected for
30 94 inserts >17 kb (**Fig. S1**), and then SMRT sequencing performed on the PacBio RS II instrument
31 95 to obtain ~96X coverage for the zebra finch (19 kb N50 read length) and ~70X for the
32 96 hummingbird (22 kb N50 read length; **Fig. S2**). The long reads were originally assembled into a
33 97 merged haplotype with an early version of the FALCON assembler [15], which we found
34 98 unintentionally introduced indels for some nucleotides that differed between haplotypes (tested
35 99 on the hummingbird; data not shown). We then re-assembled using FALCON v0.4.0 followed by
36 100 the FALCON-Unzip module [16] to prevent indel formation and generate long-range phased
37 101 haplotypes. Thus, the new assemblies, unlike the current reference assemblies, are phased
38 102 diploids. This PacBio-based sequencing and assembly approach does not link contigs into
39 103 gapped scaffolds. Scaffolding requires additional approaches, which we will report on separately
40 104 in a study comparing scaffolding technologies with these assemblies. The results presented here
41 105 were found independent of scaffolding.
42 106

43 107 For the zebra finch, our long-read approach resulted in 1159 primary haplotype contigs
44 108 with an estimated total genome size of 1.14 Gb (1.2 Gb expected; [17]) and contig N50 of 5.81
45
46
47
48
49
50
51
52
53
54
55
56
57
58
59
60
61
62
63
64
65

1
2
3
4 109 Mb, representing a 108-fold reduction in the number of contigs and a 150-fold improvement in
5
6 110 contiguity compared to the current Sanger-based reference (**Table 1A**). The diploid assembly
7 111 process produced 2188 associated, or secondary, haplotype contigs (i.e. haplotigs) with an
8
9 112 estimated length of 0.84 Gb (**Table 1A**), implying that about 75% of the genome contained
10 113 sufficient heterozygosity to be phased into haplotypes by FALCON-Unzip. Since in FALCON-
11 114 Unzip, the primary contigs are the longest path through the assembly string graph, the secondary
12
13 115 haplotigs are by definition shorter and can be more numerous, resulting in lower contiguity for
14 116 the haplotigs. Regions of the genome with very low heterozygosity remain as collapsed
15
16 117 haplotypes in the primary contigs.

17 118 The PacBio long-read assembly for the hummingbird was of similar quality, with 1076
18 119 primary contigs generating a primary haploid genome size of 1.01 Gb (1.14 Gb expected; [17]),
19
20 120 and a contig N50 of 5.36 Mb, representing a 116-fold reduction in the number of contigs and a
21 121 201-fold improvement in contiguity over the reference (**Table 1B**). The length of the assembled
22
23 122 secondary haplotigs for the hummingbird was similar to that of the primary contig backbone
24 123 (1.01 Gb; **Table 1B**) indicating that there was sufficient heterozygosity to phase most of the
25 124 diploid genome into the two haplotypes.
26
27 125

Species	Reference assembly	PacBio-based primary haplotype	Improvement	PacBio-based secondary haplotype
A. Zebra finch	Sanger-based			
Number of contigs	124,806	1,159	- 108 fold	2,188
Contig N50	38,639 bp	5,807,022 bp	+ 150 fold	2,740,176 bp
Total size	1,232,135,591 bp	1,138,770,338 bp		843,915,757 bp
B. Hummingbird	Illumina-based			
Number of contigs	124,820	1,076	- 116 fold	4,895
Contig N50	26,738 bp	5,366,327 bp	+ 201 fold	1,073,631 bp
Total size	1,105,676,412 bp	1,007,374,986 bp		1,013,746,550 bp

28
29
30
31
32
33
34
35
36
37
38
39
40
41 126
42 127 **Table 1:** *De novo* genome assembly statistics comparing intermediate-read length and short-read length
43 128 assemblies with the long-read assemblies. (A) Zebra finch intermediate-read length (Sanger-based, NCBI
44 129 accession # GCF_000151805, version 3.2.4) compared to the long-read length PacBio-based assembly.
45
46 130 (B) Anna’s hummingbird short-read length (Illumina-based, accession # GCF_000699085) compared to
47 131 the long-read length PacBio-based assembly. Improvement is calculated between the 2nd and 3rd columns
48 132 for the primary PacBio-based haplotype. The higher number of contigs in the secondary haplotype (5th
49 133 column) are a result of the arbitrary assignment of shorter haplotypes to the haplotig category.
50
51 134

52 135 **The long-read assemblies have more complete conserved protein coding genes**

53 136 To assess gene completeness, we analyzed 248 highly conserved eukaryotic genes from the
54
55 137 CEGMA human set [18, 19] in each of the assemblies. Both the PacBio-based zebra finch and
56 138 hummingbird assemblies showed improved resolution of these gene sequences, with a close to
57
58 139 doubling (~71%) for the zebra finch and 26% increase for the hummingbird in the number of
59 140 complete or near-complete (>95%) CEGMA genes assembled, compared to the references (**Fig.**
60
61
62
63
64
65

1
2
3
4 141 **1A)**. Because updating the CEGMA gene sets was recently discontinued due to lack of continued
5
6 142 funding and ease of use (<http://www.acgt.me/blog/2015/5/18/goodbye-cegma-hello-busco>), we
7 143 also searched for a set of conserved, single-copy genes from the orthoDB9 [20] gene set using
8
9 144 the recommended replacement BUSCO pipeline [21]. We observed more modest improvements
10 145 (~10%) in the number of complete genes in the zebra finch (and no change with the
11 146 hummingbird) when assessed using the BUSCO v2.0 pipeline on a set of 303 single-copy
12
13 147 conserved eukaryotic genes (**Fig. 1B**), and barely any change (1-3%) when using a newly
14 148 generated BUSCO set of 4915 avian genes (**Fig. 1C**). However, we believe that the moderate
15
16 149 increase or no change is due to the fact that much of the BUSCO gene sets were generated from
17 150 incomplete genome assemblies with short- to intermediate-length reads; for example, the 4915
18 151 protein coding avian gene set is generated mostly from the 40+ avian species that the Avian
19
20 152 Phylogenomics Project sequenced with short reads [6], including the reference hummingbird
21 153 [22]. Supporting this view, we extracted the overlapping orthologous genes in the different
22
23 154 CEGMA and BUSCO datasets, and found that the CEGMA genes are on average significantly
24 155 longer than their BUSCO counterparts (**Fig. S3**). When we manually examined genes randomly,
25 156 many of the BUSCO protein coding sequences were truncated relative to the corresponding
26
27 157 CEGMA gene and the PacBio-based assemblies (e.g. the ribosomal protein RLP24 aves BUSCO
28 158 gene is 117 a.a., whereas the CEGMA & PacBio assembly are 163 a.a.). When compared to the
29
30 159 CEGMA 303 eukaryotic set that includes several higher-quality genome assemblies, the PacBio-
31 160 based assemblies had very few fragmented genes compared to the Sanger-based and Illumina-
32
33 161 based assemblies (**Fig. 1B**). Thus, our new assemblies have the potential to upgrade the BUSCO
34 162 set to more complete and more accurately assembled genes, a conclusion supported by our
35 163 analyses below.

36 164 37 38 165 **The long-read assemblies have greater and more accurate transcriptome and regulome** 39 166 **representations**

40
41 167 To assess transcriptome gene completeness by an approach that does not depend on other
42 168 species' genomes, we aligned zebra finch brain paired-end Illumina RNA-Seq reads to the zebra
43
44 169 finch genome assemblies using TopHat2 [23]. We generated the RNA-Seq data from
45 170 microdissected RA song nuclei, a region that has convergent gene regulation with the human
46
47 171 laryngeal motor cortex (LMC) involved in speech production (**Fig. S4**; [4]). The PacBio-based
48 172 assembly resulted in a ~7% increase in total transcript read mappings compared to the Sanger-
49 173 based reference (**Fig. 2A**), suggesting more genic regions available for read alignments. This was
50
51 174 explained by a decrease in unmapped reads and increase in reads that mapped to the genome
52 175 more than once (multiple) compared to the Sanger-based reference (**Fig. 2B**), supporting the idea
53 176 that the long-read assemblies recovered more repetitive or closely related gene orthologs. The
54
55 177 PacBio assembly also resulted in ~6% more concordant aligned paired-end reads (**Fig. 2A**),
56 178 indicating a more structurally accurate assembly compared to the Sanger-based reference. RNA-
57
58 179 Seq data from the other principle brain song nuclei (HVC, LMAN, and Area X) and adjacent

1
2
3
4 180 brain regions containing multiple cell types (**Fig. S4A**; [24]) gave very similar results, with 7-
5 181 11% increased mappings to the PacBio assembled genome (not shown).

7 182 Regulatory regions have been difficult to identify in the zebra finch genome, as they are
8 183 often GC-rich and hard to sequence and assemble with short-read technologies. To assess the
9 184 regulome, we aligned HK327ac ChIP-Seq reads generated from the RA song nucleus (see
11 185 methods and [25]) to the zebra finch genome assemblies using Bowtie2 for single-end reads [26].
12 186 H3K27ac activity is generally high in active gene regulatory regions, such as promoters and
13 187 enhancers [27]. Similar to the transcriptome, there was an increase (~4%) of HK327ac ChIP-Seq
15 188 genomic reads that mapped to the PacBio-based assembly compared to the Sanger-based
16 189 reference (**Fig. 2A**). Unlike the RNA-Seq transcript reads, the ChIP-Seq genomic reads showed a
18 190 significant 10% increase in unique mapped reads with a concomitant decrease in multiple
19 191 mapped reads (**Fig. 2B**). We believe this difference is due to technical reasons in using paired-
21 192 end transcript (RNA-Seq) versus single-end genomic (ChIP-Seq) read data, as a multiple-
22 193 mapped increase with the RNA-Seq transcript data was not detected when using only one read of
23 194 each pair-end ($p=0.3$, paired t-test, $n=5$). Overall, these findings are consistent with the PacBio-
25 195 based assembly having a more complete and structurally accurate assembly for both coding and
26 196 regulatory non-coding genomic regions.

28 197 29 198 **Completion and correction of genes important in vocal learning and neuroscience research**

31 199 The genome-wide analyses above demonstrate improvements to overall genome assembly
32 200 quality using long reads, but they do not inform about real-life experiences with individual genes
33 201 where there have been challenges with assemblies. We undertook a detailed analysis of four of
34 202 our favorite genes that have been widely studied in neuroscience and in vocal learning/language
35 203 research in particular: *EGR1*, *DUSP1*, *FOXP2*, and *SLIT1*.

38 204
39 205 ***EGR1***. The early growth response gene 1 (*EGR1*) is an immediate early gene transcription factor
40 206 whose expression is regulated by activity in neurons, and is involved in learning and memory
41 207 [28]. It is up-regulated in song-learning nuclei when vocal learning birds produce song [29]; it
42 208 belongs to a large set of genes representing 10% of the transcribed genome that are up- or down-
43 209 regulated in response to activity in different cell types of the brain [25]. Studying the
44 210 mechanisms of regulation of *EGR1* and other immediate early genes has been an intensive area
45 211 of investigation [30, 31], but in all intermediate- and short-read bird genome assemblies we
46 212 examined thus far, part of the GC-rich promoter region is missing (**Fig. 3A, gap 1**).

50 213 In the zebra finch Sanger-based reference, *EGR1* is located on a 5.7 kb contig (on
51 214 chromosome 13), bounded by the gap in the GC-rich promoter region and 2 others downstream
52 215 of the gene; gaps between contigs in the published reference were given arbitrary 100 Ns [2]. We
53 216 found that the PacBio long-read assembly completely resolved all three gaps in the zebra finch
54 217 *EGR1* locus for both alleles, resulting in complete protein coding and surrounding gene bodies in
55 218 a 205.5 kb primary contig and a 129.1 kb secondary haplotig (**Fig. 3B**; **Fig. S5A**). The promoter
56 219 region gap, located 572 bp upstream of the start of the first exon, was resolved by an 804 bp
57
58
59
60
61
62
63
64
65

1
2
3
4 220 70.1% GC-rich PacBio-based sequence (**Fig. 3B, black**). In addition to the 100 Ns in the
5 reference, there were 241 bp to the left and right of this gap of low quality sequence (<QV40;
6 221 **Fig 3A, blue; 3B, red**) that was not supported by the PacBio data. For the second gap located
7 222 ~2.2 kb downstream of the *EGR1* gene, there was an adjacent 210 bp low-similarity tandem
8 223 repeat region that was also not supported by the PacBio data and also had low quality scores (**Fig**
9 224 **3A,B, gap 2**). The third 100 N gap, located ~3.5 kb downstream of the *EGR1* gene, was resolved
10 225 by 18 bp of sequence in the PacBio assembly (**Fig. 3B, gap 3**). The PacBio-based differences in
11 226 the assembly were supported by numerous long-read (>10,000 bp) molecules that extended
12 227 through the entire gene, spanning all three gaps (**Fig. S6A**). The two haplotypes were >99.8%
13 228 identical over the region shown (**Fig. 3B**), with only one synonymous heterozygous SNP in the
14 229 coding sequence (G at position 169,283 in the primary contig 405; T at position 92,478 in
15 230 secondary haplotig 405_002; tick mark in **Fig. 3B**).

16 231
17 232 In the Illumina-based hummingbird reference, *EGR1* was represented by 3 contigs
18 233 separated by 2 large gaps of 544 Ns and 1987 Ns respectively (**Fig. 3C**), in a large 2.98 Mb
19 234 scaffold. In contrast, in the PacBio-based hummingbird assembly, *EGR1* was fully resolved in a
20 235 large 810 kb contig (**Fig. 3C**). Gene prediction (using Augustus [32]) yielded a protein of the
21 236 same length as the finch *EGR1* protein (510 a.a.), and with high (93%) sequence homology (**Fig.**
22 237 **3D**). The PacBio-based assembly revealed that the larger gap in the Illumina-based assembly
23 238 harbors the beginning of the *EGR1* gene, including the entire first exon, two thirds of the first
24 239 intron, and the GC-rich promoter region (**Fig. 3C, black**). Due to this gap in the reference, the
25 240 corresponding NCBI gene prediction (accession XP_008493713.1) instead recruited a stretch of
26 241 sequence ~7 kb upstream of the gap, predicting a first exon that has no sequence homology with
27 242 *EGR1* in the PacBio-based assembly or to sequences of other species (**Fig. 3C & D**). Upstream
28 243 of this gap in the Illumina-based assembly was also a 200 bp tandem repeat that was not
29 244 supported by the PacBio sequence reads and the assembly (**Fig. 3C, red; Fig. S5B**). These
30 245 PacBio-based differences in the assembly were further validated by single-molecule Iso-Seq
31 246 mRNA long-reads of *EGR1* from a closely related species (the Ruby-throated hummingbird;
32 247 kindly provided by R. Workman & W. Timp) that fully contained both predicted exons (**Fig.**
33 248 **S6B**). The PacBio-based assembly did not generate a secondary haplotype for this region,
34 249 indicating that the two alleles are identical or nearly identical for the entire 810 kb contig in the
35 250 individual sequenced. Upstream and downstream of a high homology region that includes the
36 251 *EGR1* exons, intron, and GC-rich promoter, there was little sequence homology between the
37 252 PacBio-based hummingbird and zebra finch assemblies (**Fig. S7**).

38 253 These findings indicate that relative to the intermediate- and short-read assemblies, the
39 254 PacBio-based long-read assembly can fill in missing gaps in a previously hard-to-sequence GC-
40 255 rich regulatory region, eliminate low quality erroneous sequences and base calls at the edges of
41 256 gaps in the Sanger-based assembly, and eliminate erroneous tandem duplications adjacent to
42 257 gaps, all preventing inaccurate gene predictions. In addition, using one species as a reference to
43 258 help assemble another may not work for such a gene, as the surrounding sequence to the gene
44 259 body in these two Neoaves species is highly divergent.

1
2
3
4 260
5
6 261 *DUSPI*. The dual specificity phosphatase 1 (*DUSPI*) is also an immediate early gene, but one
7 262 that regulates the cellular responses to stress [33]. In all species examined thus far it is mostly
8
9 263 up-regulated by activity in the highly active thalamic-recipient primary sensory neurons of the
10 264 cortex (i.e. mammal cortex layer 4 cells and the comparable avian intercalated pallial cells), but
11 265 within the motor pathways, it is only up-regulated to high levels by activity in the vocal learning
12 266 circuits of vocal learners [11, 34]. This specialized regulation in vocal learning circuits has been
13
14 267 proposed to be associated with convergent microsatellite sequences found in the upstream
15 268 promoter region of the gene mainly in vocal learning species [11]. This was determined by PCR-
16
17 269 cloning of single genomic molecules from multiple species, because the reference assemblies did
18 270 not have this region properly assembled [11].

19
20 271 In the zebra finch Sanger-based reference, *DUSPI* is located on the chromosome 13
21 272 scaffold, separated in 3 contigs, with 2 gaps, all surrounded by low quality sequences (**Fig. 4A**).
22 273 The NCBI gene prediction of this assembly resulted in 4 exons generating a 322 a.a.
23 274 (XP_002192168.1), which is ~13% shorter than the *DUSPI* homologs of other species, e.g.
24 275 chicken (369 a.a., Genbank accession NP_001078828), rat (367 a.a., NP_446221), and human
25 276 (367 a.a., NP_004408). The 2 gaps coincide with the end of the first predicted exon and the
26
27 277 beginning of the third predicted exon (**Fig. 4A**). An additional gap upstream of the coding
28
29 278 sequence falls within the known microsatellite repeat region (**Fig. 4A**). The PacBio-based
30
31 279 assembly completely resolved the entire region for both alleles, in an 8.4 Mb primary contig and
32 280 an 8.0 Mb secondary haplotig (**Fig. 4B, Fig. S8A**). The Augustus gene prediction resulted in a
33
34 281 protein with 4 exons but now with a total length of 369 a.a. that was homologous across its
35 282 length to *DUSPI* of other vertebrate species (e.g., 96% with chicken GGv5 assembly, also
36 283 recently updated with long reads). Comparing the two assemblies revealed that: 1) the first exon
37
38 284 in the Sanger-based reference is truncated by 28 a.a. in the gap; 2) near the edge of that
39 285 truncation are three a.a. that appear to be errors (**Fig. 4**; residues 81, 89, and 98), as they are
40
41 286 different from genomes of other songbird species using high coverage Illumina reads (**Fig. S9A**),
42 287 with strong support in the zebra finch PacBio reads (**Fig. S9B**); 3) the second exon and adjacent
43
44 288 intron is missing a 80.8% GC-rich 0.46 kb sequence in the reference, and is instead replaced by a
45 289 1.7 kb contig of a partially repeated sequence from the microsatellite region upstream of *DUSPI*
46 290 (R' in **Fig. 4B**), part of which was erroneously recruited in the second exon of the NCBI
47
48 291 reference gene prediction (**Fig. 4D**); and 4) the microsatellite repeat itself is erroneously partially
49 292 duplicated in the reference, flanking both sides of gap 1 (R'' in **Fig. 4B**). Our PacBio phased
50
51 293 assembly revealed why both instances of R' are not identical in the reference, because they in
52 294 fact belong to the different haplotypes: the 1.7 kb contig corresponds to the upstream region in
53 295 the primary PacBio haplotype (contig 32) whereas the actual upstream region in the reference
54
55 296 corresponds to the upstream region in the secondary PacBio haplotype (contig 32_022) (**Fig.**
56 297 **4B**). This main microsatellite region is 76 bp longer (796 vs. 720 bp) in the primary haplotype,
57
58 298 and the neighboring smaller upstream microsatellite contains 3 additional 20-21 bp repeats (11
59
60
61
62
63
64
65

1
2
3
4 299 vs. 8) in the primary haplotype (**Fig. 10A**). Within the protein coding sequence there were four
5
6 300 synonymous heterozygous SNPs between haplotypes (not shown).

7 301 In the hummingbird Illumina-based assembly, the *DUSP1* region was represented by 2
8
9 302 contigs separated by a large 1005 N gap (**Fig. 4C**), on a 7 Mb scaffold. In the PacBio-based
10 303 assembly, the entire gene was fully resolved (**Fig. 4C; Fig. S8B**), in a much larger gapless 12.8
11 304 Mb contig (the second allele is fully resolved in a 3.8 Mb contig). Comparing the two assemblies
12
13 305 revealed that because of the gap in the Illumina-based reference, it lacks about half of the
14 306 *DUSP1* gene, including the first two exons and introns, and ~380 bp upstream of the start of the
15 307 gene (**Fig. 4C**). As a result, the corresponding NCBI gene prediction (XP_008496991.1)
16
17 308 recruited a sequence ~44 kb upstream predicting 46 a.a. with no sequence homology to *DUSP1*
18 309 of other species, whereas the PacBio-based assembly yielded a 369 a.a. protein with 99%
19
20 310 sequence homology to the PacBio-based zebra finch and chicken *DUSP1* (**Fig. 4D**). A 200 bp
21 311 tandem repeat in the Illumina-based assembly downstream of the gap, erroneously in exon 3, is a
22
23 312 misplaced copy of the microsatellite region (**Fig. 4C; Fig. S8B**). This is the reason why two
24 313 thirds of exon 3 is erroneously duplicated in the NCBI protein prediction (**Fig. 4D**). These
25 314 PacBio-based differences in the assembly were validated by single-molecule Iso-Seq mRNA
26
27 315 long-reads of *DUSP1* (**Fig. S11A**). The PacBio assemblies also revealed that the microsatellite
28 316 region was significantly shorter in the hummingbird (~270 bp) than the zebra finch genome
29
30 317 (~1100 bp; **Fig. S10B**).

31 318 These findings in both species demonstrate that intermediate- and short-read assemblies
32
33 319 not only have gaps with missing relevant repetitive microsatellite sequence, but that short-read
34
35 320 misassemblies of these repetitive sequences lead to erroneous protein coding sequence
36
37 321 predictions. Further, not only does the long-read assembly resolve them, but it helps generate a
38
39 322 diploid assembly that resolves allelic differences and prevents erroneous assembly duplications
40
41 323 and misplacement errors between haplotypes.

42
43 324
44 325 **FOXP2**. The forkhead box P2 (*FOXP2*) gene plays an important role in spoken-language
45
46 326 acquisition [35]. In humans, a point mutation in the protein coding binding domain in the KE
47
48 327 family [36] as well as deletions in the non-coding region of *FOXP2* [37] results in severe spoken
49
50 328 language impairments in heterozygous individuals (homozygous is lethal). In songbirds, *FOXP2*
51
52 329 expression in the Area X song nucleus is differentially regulated by singing activity and during
53
54 330 the song learning critical period, and is necessary to properly imitate song [38-40]. In mice,
55
56 331 although vocalizations are mainly innate, animals with the KE mutation demonstrate a syntax
57
58 332 apraxia-like deficit in syllable sequencing similar to that of humans [41, 42]. Thus, *FOXP2* has
59
60 333 become the most studied gene for understanding the genetic mechanisms and evolution of
61
62 334 spoken language [43], yet we find that the very large gene body of ~400 kb is incompletely
63
64 335 assembled, including in vocal learning species (**Fig. 5A**).

65
66 336 In the zebra finch Sanger-based reference, *FOXP2* is located on the chromosome 1A
67
68 337 scaffold and separated into 10 contigs (1 to 231 kb in length) with nine 100 N gaps each (**Fig.**
69
70 338 **5A**). These include 2 gaps immediately upstream of the first exon, making the beginning of the

1
2
3
4 339 gene poorly resolved. The provisional RefSeq mRNA for *FOXP2* (NM_001048263.1) contains
5 340 19 exons and encodes a 711 a.a. protein (NP_001041728.1). In the PacBio-based assembly, the
6 341 entire 400 kb gene is fully resolved for both haplotypes in 21.5 Mb and 7.6 Mb contigs,
7 342 respectively (**Fig. S12A**). As observed in the previous examples, sequences of various sizes
8
9 343 surrounding all 9 gaps in the Sanger-based reference were unsupported by the PacBio data,
10 344 resulting in a total of 2509 bp of corrected sequence in the PacBio-based primary haplotype (**Fig.**
11 345 **5B**). The two filled gaps in the upstream region and the next gap in the first intron were GC-rich
12 346 (77.6%, 66.5%, and 67.8%, respectively; **Fig. 5A,C**), indicative of the likely cause of the poor
13 347 quality Sanger-based reads (**Fig. 5D**). The DNA sequence between the two assembled PacBio
14 348 haplotypes was >99% similar across the entire 400 kb *FOXP2* gene, and identical over the
15 349 coding sequence, with differences occurring in the more complex non-coding gaps that were
16 350 difficult to sequence and assemble by the Sanger method (**Fig. 5B** *61 nucleotide differences
17 351 total). The predicted protein sequence from the PacBio-based assembly is identical to the
18 352 predicted Sanger-based reference (NP_001041728.1), with the exception of a.a. residue 42
19 353 (threonine vs. serine) (**Fig. S13A**). The PacBio nucleotide call also exists in the mRNA sequence
20 354 of another zebra finch animal in NCBI (NM_001048263.2) and in other avian species we
21 355 examined, and is thus likely a base call error in the Sanger-based zebra finch reference.

22 356 In the hummingbird Illumina-based assembly, as expected with short-read assemblies
23 357 relative to the Sanger-based zebra finch reference, the *FOXP2* gene was even more fragmented,
24 358 in 23 contigs (ranging 0.025 to 2.28 kb in lengths) with 22 gaps (**Fig. S12B**). The two largest
25 359 gaps encompass the beginning of the gene and first (non-coding) exon, resulting in
26 360 corresponding low quality predicted mRNA (XM_008496149.1). The predicted protein
27 361 (XP_008494371.1) includes an introduced correction (a.a. 402; **Fig. S13A**, X nucleotide) to
28 362 account for a genomic stop codon, and an 88 N gap within exon 6 that artificially splits the exon
29 363 into two pieces (**Fig. S13B**). In the hummingbird PacBio-based assembly, the *FOXP2* gene is
30 364 fully resolved and phased into two haplotype contigs of 3.2 Mb each (**Fig. S12B**). The erroneous
31 365 stop codon is corrected (2170128C [ctg 110] and 2183088C [ctg 110_009], instead of 841788T
32 366 [Illumina assembly scaffold 125]), and exon 6 is accurately contiguous, removing the gap and an
33 367 additional 22 bp of erroneous tandem repeat sequence adjacent to the gap (**Fig. S13B & C**). The
34 368 PacBio-based assembly also corrects three other instances of erroneous tandem duplications over
35 369 the gene region in the Illumina-based assembly, as well as removes a 462 bp stretch of sequence
36 370 adjacent to a long homonucleotide A stretch in intron 1 of the Illumina-based assembly (position
37 371 972040; **Fig. S14A**). These PacBio-based differences in the assembly were validated by single-
38 372 molecule Iso-Seq mRNA long-reads of *FOXP2* (**Fig. S11B**). The two PacBio assembled
39 373 haplotypes are >99% similar, with one heterozygous SNP (2172601T (contig 110) vs. 2185560A
40 374 (contig 110_009)) in exon 6 that is silent, and a 708 bp deletion in the secondary haplotype
41 375 (contig 110_009 [at position 2128952] relative to contig 110; **Fig. S14B**). The Illumina-based
42 376 assembly has the deleted allele.

43 377 These findings replicate those of the previously discussed genes, and in addition show
44 378 that the PacBio-based assembly can fully resolve very large genes, resolve erroneous assembled
45
46
47
48
49
50
51
52
53
54
55
56
57
58
59
60
61
62
63
64
65

1
2
3
4 379 sequences in gaps due to repeats or homonucleotide stretches, and reveal large haplotype
5 380 differences. The phased diploid assembly also avoids the possibility of large missed sequences in
6 381 a haploid only assembly due to deletions in one allele.
7
8 382

9
10 383 *SLITI*. Slit homolog 1 (*SLITI*) is a repulsive axon guidance ligand for the *ROBO1* receptor, and
11 384 is involved in circuit formation in the developing brain [44]. Recently, *SLITI* was shown to have
12 385 convergent specialized down-regulated expression compared to the surrounding brain region in
13 386 the RA song nucleus of all independently evolved vocal learning bird lineages and in the
14 387 analogous human LMC [4, 45] (**Fig. S4**), indicating a potential role of *SLITI* in the evolution and
15 388 formation of vocal learning brain circuits. A fully resolved *SLITI*, including regulatory regions,
16 389 is necessary to assess the mechanisms of its specialized regulation in vocal learning brain
17 390 regions.

21 391 In the zebra finch Sanger-based reference, *SLITI* is located on chromosome 6, split
22 392 among 8 contigs with 7 gaps, and 7 additional contigs and gaps surrounding the ~40 kb gene
23 393 (**Fig. 6A**). The *SLIT1* gene is complex, with over 35 exons. We noted an incomplete predicted
24 394 protein of the reference (XP_012430014.1) relative to some other species (chicken
25 395 [NM_001277336.1], human [NM_003061.2], and mouse [NM_015748.3]), and our *de novo* gene
26 396 predictions from the reference also resulted in a truncated protein with two missing exons (**Fig.**
27 397 **6B**). The PacBio-based assembly fully resolved the gene region, in two alleles on 15.7 Mb and
28 398 5.6 Mb contigs, respectively, and completely recovered all 35+ exons (**Fig. S15A**). Similar to
29 399 above, reference sequences flanking the gaps were found to be erroneous and corrected, and an
30 400 erroneous tandem duplication was also corrected (not shown). Filling in these gaps recovered the
31 401 two missing exons: exon 1 within a 1 kb region of sequence in the PacBio-based assembly that is
32 402 75% GC-rich, replacing 390 bp of erroneous gap-flanking sequence; and exon 35 adjacent to a
33 403 gap (**Fig. 6A,B**). A predicted exon upstream of exon 1 in a repeat region was not supported (**Fig.**
34 404 **6A,B**). The PacBio-based assembly thereby generates a complete *SLITI* gene prediction of 1538
35 405 a.a. (**Fig. 6B**). The gene is heterozygous in the individual, with 3 codon differences between the
36 406 two alleles (**Fig. 6B**, positions 90, 1006, and 1363, respectively), and an additional 24 silent
37 407 heterozygous SNPs across the coding region. The two alleles were phased along the entire length
38 408 of the gene.

46 409 In the hummingbird Illumina-based assembly, the *SLITI* gene is separated on 9 contigs
47 410 with 8 gaps ranging in length from 91 to 1018 bp, comprising 3320 bp of missing sequence, or
48 411 5.3% of the gene region (**Fig. S15B**). The PacBio-based assembly fully resolved and phased
49 412 *SLITI* into haplotypes on 9.9 Mb contigs (**Fig. S15B**). The resulting protein of 1538 a.a. has high
50 413 homology to the zebra finch PacBio-based *SLITI* (95% a.a. identity; **Fig. 6B**) and the individual
51 414 is homozygous for the *SLIT1* protein. Comparisons revealed that as with the Sanger-based
52 415 reference, the first exon (68 a.a.) is missing completely in the Illumina-based assembly (**Fig. 6B**),
53 416 corresponding to a gap of 495 Ns, which the PacBio-based assembly replaced by a 567 bp 76%
54 417 GC-rich sequence (**Fig. S15B**). In addition, there were two sequence errors in the Illumina-based
55
56
57
58
59
60
61
62
63
64
65

1
2
3
4 418 assembly, which resulted in erroneous amino acid predictions in the SLIT1 protein (**Fig. 6B**,
5 419 positions 118 and 1381, respectively).

7 420 These findings demonstrate that long-read assemblies can fully resolve a complex multi-
8 421 exon gene, as well as have a higher base-call accuracy than Sanger- or Illumina-based reads in
9 422 difficult to sequence regions, including exons, leading to higher protein-coding sequence
10 423 accuracy.
11 424

14 425 **Other genes.** We have manually compared several dozen other genes between the different
15 426 assemblies, and found in all cases investigated that errors in the Sanger-based and Illumina-based
16 427 assemblies were corrected in the PacBio-based long-read assemblies. These genes included other
17 428 immediate early gene transcription factors, other genes in the *SLIT* and *ROBO* gene families, and
18 429 the *SAP30* gene family, which all had the same types of errors in the genes discussed above. In
19 430 addition, we also found cases where genes were missing from the Sanger-based zebra finch or
20 431 Illumina-based hummingbird assemblies entirely, and could have been interpreted as lost in these
21 432 species. These included the DNA methyltransferase enzyme *DNMT3A* missing in the Sanger-
22 433 based finch assembly and *DRD4* missing in the hummingbird assembly [10], with both fully
23 434 represented in the PacBio-based assemblies. We also noted cases where an assembled gene was
24 435 incorrectly localized on a scaffold in the Sanger-based assembly whose synteny was corrected
25 436 with the PacBio-based assembly, such as the vasopressin receptor AVPR1B, which will be
26 437 reported on in more detail separately. Data for these types of errors were not shown due to space
27 438 limitations, but they offer further examples of the important improvements of PacBio long-read
28 439 technology for generating more accurate genome assemblies.
29
30
31
32
33
34
35
36
37

38 442 **Discussion and Conclusions**

39 443
40 444 Although the intermediate-read and short-read assemblies had correct sequences and assembled
41 445 regions in terms of total base pairs covered, the long-read assemblies revealed numerous errors
42 446 within and surrounding many genes. These errors are not simply in so-called “junk” intergenic
43 447 repetitive DNA known to be hard to assemble with short reads [46, 47], but within functional
44 448 regions of genes. The assemblers for the short reads sometimes take a repetitive sequence, some
45 449 in functional repetitive regulatory regions, and insert them in a non-repetitive region of a gene,
46 450 resulting in an error. Some of these assembly errors and gaps in the sequences lead to gene and
47 451 protein coding sequence prediction errors, sometimes recruiting completely wrong sequence in
48 452 the protein.

53 453 The PacBio-based long-read assemblies corrected these problems, and for the first time
54 454 resolved gene bodies of all the genes we examined into single, contiguous, gap-less sequences.
55 455 The phasing of haplotypes, although initially done to prevent a computationally introduced indel
56 456 error, reveal how important phasing is to prevent assembly and gene prediction errors. Thus far,
57 457 we have not seen an error (i.e. difference) in the genes we examined in the PacBio-based long-
58
59
60
61
62
63
64
65

1
2
3
4 458 read assembly relative to the other assemblies that was supported by single sequenced genomic
5 459 DNA molecules, RNA-Seq and Iso-Seq mRNA molecules, or other independent evidence. With
6 460 these improvements, we now, for the first time, have complete and accurate assembled genes of
7 461 interest that we now can pursue further without the need to individually and arduously clone,
8 462 sequence, and correct the assemblies one gene at a time.

11 463 Our study highlights the value of maintaining frozen tissue or cells of the individuals
12 464 used to create previous reference genomes, as we could only discover some of the errors (e.g.
13 465 caused by haplotype differences) by long-read *de novo* genome assemblies of the same
14 466 individual used to create the reference. We are now using these PacBio-based assemblies with
15 467 several groups and companies as starting assemblies for scaffolding into phased, diploid,
16 468 chromosome-level zebra finch and hummingbird assemblies to upgrade the references, which
17 469 will be reported on separately. However, even without scaffolding, these more highly contiguous
18 470 assemblies will be helpful to researchers to extract more accurate assemblies of their genes of
19 471 interests, saving a great amount of time and energy, while adding new knowledge and biological
20 472 insights necessary for understanding gene structure, function, and evolution.

25 473 26 474 27 475 **Materials & Methods**

28 476 29 477 **DNA isolation**

30 478 For both the zebra finch and hummingbird, frozen muscle tissue from the same animals used to
31 479 create the Sanger-based [2] and Illumina-based [6] references, respectively, was processed for
32 480 DNA isolation using the KingFisher Cell and Tissue DNA Kit (97030196). Tissue was
33 481 homogenized in 1 ml of lysis buffer in M tubes (Miltenyi Biotec) using the gentleMACS™
34 482 Dissociator at the Brain 2.01 setting for 1 minute. The cell lysate was treated with 40 ul of
35 483 protease K (20mg/ml) and incubated overnight. DNA was purified using the KingFisher Duo
36 484 system (5400100) using the built in KFDuoC_T24 DW program.

37 485 38 486 **Library preparation and sequencing**

39 487 For the zebra finch, two samples were used for library construction. Each DNA sample was
40 488 mechanically sheared to 60 kb using the Megaruptor system (Diagenode). Then >30 kb libraries
41 489 were created using the SMRTbell Template Prep Kit 1.0 (Pacific Biosciences), which includes a
42 490 DNA Damage Repair step after size selection. Size selection was made for 15 kb for the first
43 491 sample and 20 kb for the second sample, using a Blue Pippin instrument (Sage Science)
44 492 according to the protocol “Procedure & Checklist – 20 kb Template Preparation Using
45 493 BluePippin Size-Selection System”. For the hummingbird, 70 ug of input DNA was
46 494 mechanically sheared to 35 and 40 kb using the Megaruptor system, a SMRTbell library
47 495 constructed, and size selected to > 17 kb with the BluePippin. Library quality and quantity were
48 496 assessed using the Pippin Pulse field inversion gel electrophoresis system (Sage Science), as well
49 497 as with the dsDNA Broad Range Assay kit and Qubit Fluorometer (Thermo Fisher).

1
2
3
4 498 SMRT sequencing was performed on the Pacific Biosciences RS II instrument at Pacific
5 Biosciences using an on plate concentration of 125 pM, P6-C4 sequencing chemistry, with
6 499 magnetic bead loading, and 360 minute movies. A total of 124 SMRT Cells were run for the
7 500 zebra finch and 63 SMRT Cells for the hummingbird. Sequence coverage for the zebra finch was
8 501 ~96 fold, with half of the 114 Gb of data contained in reads longer than 19 kb. For the
9 502 hummingbird, coverage was ~70 fold, with half of the 40.4 Gb of data contained in reads longer
10 503 than 22 kb (Fig. S2).
11
12
13
14 505

15 506 **Assembly**

16 507 Assemblies were carried out using FALCON v0.4.0 followed by the FALCON-Unzip module
17 508 [16]. FALCON is based on a hierarchical genome assembly process [48]. It constructs a string
18 509 graph from error-corrected PacBio reads that contains ‘haplotype-fused’ genomic regions as well
19 510 as “bubbles” that capture divergent haplotypes from homologous genomic regions. The
20 511 FALCON-Unzip module then assigns reads to haplotypes using heterozygous SNP variants
21 512 identified in the FALCON assembly to generate phased contigs corresponding to the two alleles.
22 513 The diploid nature of the genome is thereby captured in the assembly by a set of primary contigs
23 514 with divergent haplotypes represented by a set of additional contigs called haplotigs. Genomic
24 515 regions with low heterozygosity are represented as collapsed haplotypes in the primary contigs.
25 516 Genome assemblies were run on an SGE-managed cluster using up to 30 nodes, where each node
26 517 has 512 Gb of RAM distributed over 64 slots. The same configuration files were used for both
27 518 species (Additional file 1). Three rounds of contig polishing were performed. For the first round,
28 519 as part of the FALCON-Unzip pipeline, primary contigs and secondary haplotigs were polished
29 520 using haplotype-phased reads and the Quiver consensus caller. For the second and third rounds
30 521 of polishing, using the “resequencing” pipeline in SMRTlink v3.1, primary contigs and haplotigs
31 522 were concatenated into a single reference and BLASR was used to map all raw reads back to the
32 523 assembly, followed by consensus calling with Arrow.
33
34
35
36
37
38
39
40
41 524

42 525 **Genome completeness**

43 526 To assess quality and completeness of the assemblies, we used a set of 248 highly conserved
44 527 eukaryotic genes from the CEGMA human set [19] and located them in each of the assemblies
45 528 compared in this study. Briefly, the CEGMA human peptides were aligned to each genome using
46 529 genblastA [49]. The regions showing homology were then used to build gene models with
47 530 exonerate [50] which were then assessed for frameshifts using custom shell scripts. In addition,
48 531 we queried each genome for a set of 303 eukaryotic conserved single-copy genes as well as from
49 532 4915 conserved single-copy genes from 40 different avian species using the BUSCOv2.0
50 533 pipeline [21].
51
52
53
54

55 534 To compare protein amino acid sequence size between the CEGMA and BUSCO
56 535 datasets, we performed blastp of each CEGMA sequence against the ancestral proteins of the
57 536 target BUSCO dataset. We took the single best hit with an e-value cut off of 0.001 and extracted
58 537 the CEGMA and BUSCO protein length values. We then ran a one-sided paired Wilcoxon
59
60
61
62
63
64
65

1
2
3
4 538 signed-rank test of the two lengths for each protein.
5
6 539

7 540 **Gene prediction**

8 541 Gene predictions for the zebra finch PacBio-based assembly were conducted by running
9 542 Augustus gene prediction software (v3.2.2, [32]) on the contigs, and incorporating the Illumina
10 543 short read RNA-Seq brain data aligned with Tophat2 (v2.0.14, [23]) as hints for possible gene
11 544 structures. The data consisted of 146,126,838 paired-end reads with an average base quality
12 545 score of 36. Augustus produces a distribution of possible gene models for a given locus and
13 546 models that are supported by our RNA-Seq data are given a “bonus” while the gene models not
14 547 supported by RNA-Seq data are given a “penalty”. This results in the gene model most informed
15 548 by biological data being selected as the most likely gene model for that locus.

16 549 We did not have Illumina transcriptome data for Anna’s hummingbird, so standard
17 550 Augustus gene prediction (v3.2.2) was used with both chicken and human training background to
18 551 determine the sequence predictions of the genes examined. The human-based predictions
19 552 captured more of the divergent 5’ ends of the longer genes (*SLIT1* and *FOXP2*) than the chicken-
20 553 based predictions, so a combination of both were used to produce the final sequences in this
21 554 manuscript.

22 555
23 556 **RNA-Seq**

24 557 RNA sequencing was centered around vocal learning brain regions in the zebra finch and will be
25 558 described in more detail in a later publication. We utilized our data here for population analyses
26 559 of assembly quality and for initial annotations. In brief, following modifications of a previously
27 560 described protocol [25], nine adult male zebra finches were isolated in soundproof chambers for
28 561 12 hours in the dark to obtain brain tissue from silent animals. Then brains were dissected from
29 562 the skull and sectioned to 400 microns using a Stoelting tissue slicer (51415). The sections were
30 563 moved to a petri dish containing cold PBS with proteinase inhibitor cocktail (11697498001).
31 564 Under a dissecting microscope (Olympus MVX10), the four principle song nuclei (Area X,
32 565 LMAN, HVC, and RA) as well as their immediate adjacent brain regions were microdissected
33 566 using 2mm fine scissors and placed in microcentrifuge tubes. The samples were stored at -80
34 567 °C. Then RNA was isolated and quantified, and samples of two birds were then pooled for each
35 568 replicate, resulting in 5 replicates (one single animal in one). RNA was converted to cDNA and
36 569 library preparation was performed using the NEXTflex™ Directional RNA-Seq Kit (Illumina)
37 570 and paired-end reads were sequenced on an Illumina HiSeq 2500 system. Adapters and poor
38 571 quality bases (<30) were trimmed using fastq-mcf from the ea-utilities package, and reads were
39 572 aligned to assemblies using Tophat2 (v2.0.14).

40 573
41 574 **Chip-Seq**

42 575 Three adult male zebra finches were treated as above, the brains dissected, and the RA and
43 576 surrounding arcopallium of each bird was then processed individually using the native ChIP
44 577 protocol described in [51] with an H3K27ac antibody (Ab#4729). The DNA libraries were
45
46
47
48
49
50
51
52
53
54
55
56
57
58
59
60
61
62
63
64
65

1
2
3
4 578 prepared using the MicroPlex Library Preparation Kit v2 (C05010012). 50 bp single-end
5 579 sequencing was done on the Illumina HiSeq 4000 system. The reads were aligned to the
6 580 assemblies using Bowtie2 (v2.2.9, [26]). More detail will be provided in a later publication
7 581 focusing on vocal learning brain regions.
8
9

10 582 11 583 **Comparative analyses between assemblies for individual genes**

12 584 The Sanger-based reference zebra finch assembly in the UCSC browser and the Illumina-based
13 585 reference Anna's Hummingbird in Avianbase (<http://avianbase.narf.ac.uk/index.html>), and both
14 586 in NCBI where used for comparing with the Pacbio assembly. In the UCSC browser, there are
15 587 two annotations, one from 2008 (<http://genome.ucsc.edu/cgi-bin/hgGateway?db=taeGut1>) and
16 588 the other from 2013 (<http://genome.ucsc.edu/cgi-bin/hgGateway?db=taeGut2>), with some
17 589 differences between them. Our findings were similar, although not always identical, with both
18 590 annotations, with errors being present in both annotations based on the Pacbio assembly. The
19 591 nucleotide quality score tract was only available in the 2008 browser.

20 592 Multiple species sequence alignments were done with BioEdit v7.2.5
21 593 (<http://www.mbio.ncsu.edu/bioedit/bioedit.html>) [52]; Dotplots of alignments were generated
22 594 with Gepard v1.4 (<http://cube.univie.ac.at/gepard>) [53]; Alignments of raw SMRT genome reads
23 595 to the assembled genomes were done with Blasr, which is part of SMRTLink software from
24 596 Pacbio; Iso-Seq reads were aligned with GMAP (<http://research-pub.gene.com/gmap/>) [54].
25
26
27
28
29
30

31 597 32 598 33 599 **Availability of data**

34 600 This Whole Genome Shotgun project has been deposited at DDBJ/ENA/GenBank under
35 601 BioProject PRJNA368994. The zebra finch accession number is MUGN00000000 and SRA for
36 602 raw reads is SRS1954332. The Anna's Hummingbird accession number is MUGM00000000 and
37 603 SRA is SRP061272.
38
39
40

41 604 42 605 **Competing interest**

43 606 Jonas Korch, Sarah Kingan, Chen-Shan Chin are full-time employees at Pacific Biosciences, a
44 607 company developing single-molecule sequencing technologies.
45
46
47

48 608 49 609 **Funding**

50 610 This work was supported by HHMI funds to E.D.J. and PacBio funds to J. K.
51 611

52 612 53 613 **Author contributions**

54 614 J.K. and E.D.J. designed the project and wrote the manuscript; C.S.C. and S.K. carried out
55 615 genome assemblies; J.K., G.G. and S.K. conducted analyses on single genes as well as CEGMA
56 616 and BUSCO analyses; G.G. and J-N.A. conducted RNA-Seq experiments, L.C. conducted Chip-
57 617 Seq experiments; J.H. processed samples; and all authors contributed to writing and editing the
58
59
60
61
62
63
64
65

1
2
3
4
5
6
7
8
9
10
11
12
13
14
15
16
17
18
19
20
21
22
23
24
25
26
27
28
29
30
31
32
33
34
35
36
37
38
39
40
41
42
43
44
45
46
47
48
49
50
51
52
53
54
55
56
57
58
59
60
61
62
63
64
65

618

Acknowledgements

620 We thank Art Arnold for sending us the carcass with tissue used to create the original Sanger-
621 based zebra finch assembly, and Claudio Mello and Peter Lovell again for their previous capture
622 of the hummingbird used for the reference assembly. We thank the PacBio sequencing (Christine
623 Lambert, Jill Muehling, Primo Baybayan) and assembly (Matthew Seetin, Richard Hall, Jane
624 Landolin, Lawrence Hon) teams for help with sequencing and assembly, and Winston Timp and
625 Rachael Workman for early access to their Iso-Seq reads of the Ruby-throated hummingbird. We
626 thank Alejandro Burga for noticing indel errors in the original PacBio haploid assembly that lead
627 us work with others to find a correction with phasing, and several members of the Jarvis lab
628 (Mathew Biegler, Ha Na Choe, and Constantina Theofanopoulou) and Asher Haug-Baltzell for
629 help with manual analyses of gene models between the assemblies. Finally, we thank members
630 of the G10K and B10K consortiums for valuable discussions on metrics of genome assembly
631 quality.

632

633

Additional Files

634 Supporting data is included in supplementary figures S1-S15.

636

Figure legends

Figure 1. Gene completeness within assemblies. (A) Comparison to a 248 highly conserved core CEGMA eukaryote gene set using human genes [19], between the Sanger-based zebra finch and Illumina-based Anna's hummingbird references and their respective PacBio-based assemblies. We used a more stringent cut-off ($> 95\%$) for completeness than usually done ($> 90\%$). Gent count is the percentage of genes in each of the assemblies that met this criterion. (B) Comparison to a 303 single-copy conserved eukaryotic BUSCO gene set [21]. Complete is $\geq 95\%$ complete; fragmented is $< 95\%$ complete; missing is not found. (C) Comparison to 4915 single-copy conserved genes from the avian BUSCO gene [21].

Figure 2. Transcriptome and regulome representation within assemblies. (A) Percentage of RNA-Seq and H3K27Ac ChIP-Seq reads from the zebra finch RA song nucleus mapped back to the zebra finch Sanger-based and PacBio-based genome assemblies. (B) Pie charts of the distributions of the RNA-Seq reads mapped to the zebra finch genome assemblies. (C) Pie charts of the distribution of ChIP-Seq reads mapped to the zebra finch genome assemblies. * $p < 0.05$; ** $p < 0.002$; *** $p < 0.0001$; paired t-test within animals between assemblies; $n = 5$ RNA-Seq and $n = 3$ ChIP-Seq independent replicates from different animals.

Figure 3. Comparison of *EGR1* assemblies. (A) UCSC Genome browser view of the Sanger-based zebra finch *EGR1* assembly, highlighting (from top to bottom) four contigs (light and dark brown) with three gaps, GC percent, nucleotide quality score (blue), RefSeq gene prediction (purple), and areas of repeat sequences. (B) Summary comparison of the Sanger-based and PacBio-based zebra finch assemblies, showing in the latter filling the gaps (black) and correcting erroneous reference sequences surrounding the gaps (red). Tick mark is a synonymous heterozygous SNP in the coding region between the primary (1) and secondary (2) haplotypes. Panels A and B are of the same scale. (C) Comparison of the hummingbird Illumina- and PacBio-based assemblies, showing similar corrections that further lead to a correction in the protein coding sequence prediction (blue). (D) Multiple sequence alignment of the *EGR1* protein for the four assemblies (two zebra finch and two hummingbird) in B and C, showing corrections to the Illumina-based hummingbird protein prediction by the PacBio-based assembly.

Figure 4. Comparison of *DUSP1* assemblies. (A) UCSC Genome browser view of the Sanger-based zebra finch *DUSP1* assembly, highlighting four contigs with three gaps, GC percent, nucleotide quality score, Blat alignment of the NCBI gene prediction (XP_002193168.1, blue), and repeat sequences. (B) Resolution of the region by the PacBio-based zebra finch assembly, filling the gaps (black) and correcting erroneous reference sequences in repeat regions (red) and gene predictions (blue). Panels A and B are of the same scale. (C) Resolution and correction to the hummingbird Illumina-based assembly with the PacBio-based assembly (same color scheme as in B). (D) Multiple sequence alignment of the *DUSP1* protein for the four assemblies in B and

1
2
3
4 677 C, showing numerous corrections to the Sanger-based and Illumina-based protein predictions by
5 678 both PacBio-based assemblies.
6
7 679

8 680 **Figure 5.** Comparison of *FOXP2* assemblies. (A) UCSC Genome browser view of the Sanger-
9 681 based zebra finch *FOXP2* assembly, highlighting 10 contigs with 9 gaps, GC percent, nucleotide
10 682 quality score, RefSeq gene prediction, and repeat sequences. (B) Table showing the number of
11 683 resolved and corrected erroneous base pairs in the gaps by the PacBio-based primary and
12 684 secondary haplotype assemblies; * indicates differences between haplotypes. (C) Dot plot of the
13 685 Sanger-based reference (x-axis) and the PacBio-based primary assembly (y-axis) corresponding
14 686 to the three GC-rich region gaps immediately upstream and surrounding the first exon of the
15 687 *FOXP2* gene. (D) Schematic summary of corrections to the three gaps shown in C, in the two
16 688 haplotypes of the PacBio-based assembly. The protein coding sequence alignments are in Figure
17 689 S13A.
18
19
20
21
22
23

24 691 **Figure 6.** Comparison of *SLIT1* assemblies. (A) UCSC Genome browser view of the Sanger-
25 692 based zebra finch *SLIT1* assembly, highlighting 15 contigs with 14 gaps, GC percent, nucleotide
26 693 quality score, NCBI *SLIT1* gene prediction (XP_012430014.1, blue), and repeat sequences. Red
27 694 circles, gaps that correspond to the missing exon 1 and part of the missing exon 35, respectively.
28 695 (B) Multiple sequence alignment comparison of the *SLIT1* protein for the four assemblies
29 696 compared, including the two different haplotypes from the PacBio-based zebra finch assembly
30 697 (rows 2 and 3).
31
32
33
34

35 699 **Supplementary Figure S1.** DNA isolation, library construction, and size selection. (A) Pulsed-
36 700 field gel showing original size of starting genomic DNA (lane 3), the sheared DNA (1), and the
37 701 size selected library (2). (B) Bioanalyzer trace before (blue) and after (red) library size selection
38 702 for fragments > 17 kb.
39
40
41

42 704 **Supplementary Figure S2.** Read and insert length distributions. (A, B) Sequence read length
43 705 distributions from SMRT cell sequencing for both species. (C, D) Sequenced DNA insert length
44 706 distributions from SMRT cell sequencing for both species.
45
46
47

48 708 **Supplementary Figure S3.** Box plots comparing protein coding sequence lengths of
49 709 orthologous proteins between the CEGMA and BUSCO eukaryotic and avian datasets. ** $p <$
50 710 0.001; *** $p <$ 0.0001, one-sided paired Wilcoxon signed-rank test, prediction of the proteins
51 711 being longer in CEGMA datasets.
52
53

54 713 **Supplementary Figure S4.** Vocal learning and adjacent brain regions in songbirds used for
55 714 RNA-Seq and ChIP-Seq analyses, and comparison with humans. (A) Drawing of a zebra finch
56 715 male brain section showing specialized vocal learning pathway and associated profiled song
57 716 nuclei RA, HVC, LMAN, and Area X. (B) Drawing of a human brain section showing spoken-
58
59
60
61
62
63
64
65

1
2
3
4 717 language pathway and analogous brain regions. Black arrows, posterior vocal motor pathway;
5 718 White arrows, anterior vocal learning pathway; Dashed arrows, connections between the two
6 719 pathways; Red arrow, specialized direct projection from forebrain to brainstem vocal motor
7 720 neurons in vocal learners. Italicized letters adjacent to the song and speech regions indicates
8 721 regions (in songbirds) that show mainly show motor (*m*), auditory (*a*), equally both motor and
9 722 auditory (*m/a*) neural activity or activity-dependent gene expression. Figure from [55] and [4].
10 723

11 724 *Abbreviations:* A1-L4, primary auditory cortex – layer 4; Am, nucleus ambiguous; Area X, a
12 725 vocal nucleus in the striatum; aSt, anterior striatum vocal region; aT, anterior thalamus speech
13 726 area; Av, avalanche; aDLM, anterior dorsolateral nucleus of the thalamus; DM, dorsal medial
14 727 nucleus of the midbrain; HVC, a vocal nucleus (no abbreviation); L2, auditory area similar to
15 728 human cortex layer 4; LSC, laryngeal somatosensory cortex; LMC, laryngeal motor cortex;
16 729 MAN, magnocellular nucleus of the anterior nidopallium; MO, oval nucleus of the anterior
17 730 mesopallium; Nif, interfacial nucleus of the nidopallium; PAG, peri-aqueductal gray; RA, robust
18 731 nucleus of the arcopallium; v, ventricle space
19 732

20 733 **Supplementary Figure S5.** Dot plot of sequence comparisons for genome assemblies of the
21 734 *EGR1* region. (A) Comparison of zebra finch PacBio-based versus Sanger-based assemblies for
22 735 the region containing *EGR1*, showing the GC-rich promoter region and closing and corrections
23 736 of gaps for the PacBio-based assembly. (B) Comparison of hummingbird Illumina-based versus
24 737 PacBio-based assemblies for the region containing *EGR1*, showing an erroneous tandem
25 738 duplication in the Illumina-based assembly and closing of gaps for the PacBio-based assembly.
26 739

27 740 **Supplementary Figure S6.** Single SMRT genomic reads and Iso-Seq mRNA reads supporting
28 741 PacBio *EGR1* assembly. (A) Zebra finch PacBio SMRT reads (rows) mapped against the zebra
29 742 finch PacBio assembly (contig 405, entire *EGR1* region, same as Fig. 3A). Reads are shaded by
30 743 length (>10 kb reads = black). (B) Example of a single Ruby-throated hummingbird Iso-Seq read
31 744 mapped against Illumina-based (top) and PacBio-based (bottom) Anna's hummingbird genome
32 745 assemblies using GMAP. Note the first exon (blue) which is present in the Iso-Seq read is
33 746 missing in the Illumina-based assembly, but present in the PacBio-based assembly.
34 747

35 748 **Supplementary Figure S7.** Dot plot of sequence comparison for the PacBio-based hummingbird
36 749 and zebra finch *EGR1* region assemblies. Note regions of high species conservation and
37 750 divergence surrounding *EGR1*. Blue box, location of the *EGR1* exons and intron.
38 751

39 752 **Supplementary Figure S8.** Dot plot comparisons for *DUSP1* region assemblies. (A)
40 753 Comparison of the Sanger-based and PacBio-based zebra finch *DUSP1* region assemblies,
41 754 showing problems in the Sanger-based assembly with microsatellite repeats. (B) Comparison of
42 755 the Illumina-based and PacBio-based hummingbird *DUSP1* region assemblies, showing a large
43
44
45
46
47
48
49
50
51
52
53
54
55
56
57
58
59
60
61
62
63
64
65

1
2
3
4 756 gap including the microsatellite region and the beginning of the gene, and an erroneous tandem
5 757 duplication in the Illumina-based assembly.
6
7 758
8
9 759 **Supplementary Figure S9.** Pacbio correction of base call errors found in Sanger reference (A)
10 760 Confirmation of the PacBio sequence in the three locations different from the zebra finch Sanger
11 761 reference by alignments to *DUSP1* sequences of other songbirds. (B) PacBio reads (rows)
12 762 corresponding to the genomic region in *DUSP1* that differs in the three locations from the zebra
13 763 finch Sanger reference, resulting in a.a. changes. The codons in question are highlighted.
14
15 764
16
17 765 **Supplementary Figure S10.** Dot plot comparison of assemblies for the *DUSP1* microsatellite
18 766 region. (A) Differences in the microsatellite region upstream of the *DUSP1* protein coding
19 767 sequence between the primary and the secondary haplotypes in the fully assembled zebra finch
20 768 PacBio-based assembly. (B) Differences in microsatellites region upstream of *DUSP1* between
21 769 the zebra finch and hummingbird in the fully assembled PacBio-based assemblies.
22
23 770
24
25 771 **Supplementary Figure S11.** Single Iso-Seq mRNA reads supporting Pacbio assemblies. (A)
26 772 Full-length PacBio mRNA sequence Iso-Seq ruby throated hummingbird reads for *DUSP1*
27 773 aligned against the exons of the corresponding primary contigs from Anna's hummingbird
28 774 Illumina (top panel) and PacBio (bottom panel) assemblies. (B) Similar alignments for *FOXP2*
29 775 IsoSeq reads.
30
31 776
32
33 777 **Supplementary Figure S12.** Dot plot comparison of assemblies for the *FOXP2* region. (A)
34 778 zebra finch, (B) hummingbird.
35
36 779
37
38 780 **Supplementary Figure S13.** (A) Multiple sequence alignment of the *FOXP2* protein for the four
39 781 assemblies (two zebra finch and two hummingbird) compared in this study, showing correction
40 782 of a nucleotide error in the Sanger-based zebra finch assembly, and correction of an erroneous
41 783 stop codon (x) in the Illumina-based hummingbird assembly. Note an extra 18 a.a. stretch in the
42 784 hummingbird sequence validated by gene prediction of both assemblies, that was not present in
43 785 the zebra finch. (B) Missing 88bp of sequence in exon 6 of Illumina-based assembly. (C)
44 786 Resolution of exon 6 in Pacbio-based assembly, also revealing a SNP.
45
46 787
47
48 788 **Supplementary Figure S14.** Large regional correction made by the PacBio diploid assembly.
49 789 (A) Correction of an erroneous stretch of 462 bp in the first intron of *FOXP2* in the hummingbird
50 790 Illumina assembly by the PacBio assembly. (B) Dot plot of haplotype variation in the *FOXP2*
51 791 gene revealed by the PacBio diploid assembly: a 708 bp deletion in the secondary haplotype
52 792 contig relative to the primary contig.
53
54 793
55
56 794 **Supplementary Figure S15.** Dot plot comparison of assemblies for the *SLIT1* region. (A) zebra
57 795 finch, (B) hummingbird.
58
59 796
60
61
62
63
64
65

References

1. Hillier LW, Miller W, Birney E, Warren W, Hardison RC, Ponting CP, Bork P, Burt DW, Groenen MA, Delany ME, et al: **Sequence and comparative analysis of the chicken genome provide unique perspectives on vertebrate evolution.** *Nature* 2004, **432**:695-716.
2. Warren WC, Clayton DF, Ellegren H, Arnold AP, Hillier LW, Kunstner A, Searle S, White S, Vilella AJ, Fairley S, et al: **The genome of a songbird.** *Nature* 2010, **464**:757-762.
3. Shi Z, Luo G, Fu L, Fang Z, Wang X, Li X: **miR-9 and miR-140-5p target FoxP2 and are regulated as a function of the social context of singing behavior in zebra finches.** *J Neurosci* 2013, **33**:16510-16521.
4. Pfenning AR, Hara E, Whitney O, Rivas MV, Wang R, Roulhac PL, Howard JT, Wirthlin M, Lovell PV, Ganapathy G, et al: **Convergent transcriptional specializations in the brains of humans and song-learning birds.** *Science* 2014, **346**:1256846.
5. Zhang GJ, Jarvis ED, Gilbert MTP: **A flock of Genomes.** *Science* 2014, **346**:1308-1309.
6. Zhang GJ, Li C, Li QY, Li B, Larkin DM, Lee C, Storz JF, Antunes A, Greenwold MJ, Meredith RW, et al: **Comparative genomics reveals insights into avian genome evolution and adaptation.** *Science* 2014, **346**:1311-1320.
7. Jarvis ED, Mirarab S, Aberer AJ, Li B, Houde P, Li C, Ho SY, Faircloth BC, Nabholz B, Howard JT, et al: **Whole-genome analyses resolve early branches in the tree of life of modern birds.** *Science* 2014, **346**:1320-1331.
8. Joseph L, Buchanan KL: **A quantum leap in avian biology.** *Emu* 2015, **115**:1-5.
9. Kraus RHS, Wink M: **Avian genomics: fledging into the wild!** *Journal of Ornithology* 2015, **156**:851-865.
10. Haug-Baltzell A, Jarvis ED, McCarthy FM, Lyons E: **Identification of dopamine receptors across the extant avian family tree and analysis with other clades uncovers a polyploid expansion among vertebrates.** *Frontiers in Neuroscience* 2015, **9**.
11. Horita H, Kobayashi M, Liu WC, Oka K, Jarvis ED, Wada K: **Specialized Motor-Driven *dusp1* Expression in the Song Systems of Multiple Lineages of Vocal Learning Birds.** *PLoS ONE* 2012, **7**:e42173.
12. Roberts RJ, Carneiro MO, Schatz MC: **The advantages of SMRT sequencing.** *Genome Biol* 2013, **14**:405.
13. Bradnam KR, Fass JN, Alexandrov A, Baranay P, Bechner M, Birol I, Boisvert S, Chapman JA, Chapuis G, Chikhi R, et al: **Assemblathon 2: evaluating de novo methods of genome assembly in three vertebrate species.** *Gigascience* 2013, **2**:10.
14. Gordon D, Huddleston J, Chaisson MJ, Hill CM, Kronenberg ZN, Munson KM, Malig M, Raja A, Fiddes I, Hillier LW, et al: **Long-read sequence assembly of the gorilla genome.** *Science* 2016, **352**:aae0344.
15. **FALCON** **assembler**
[<https://github.com/PacificBiosciences/FALCON/commit/a1180264c3c7d2de1c5eb55b3663dce093354dd7>]
16. Chin CS, Peluso P, Sedlazeck FJ, Nattestad M, Concepcion GT, Clum A, Dunn C, O'Malley R, Figueroa-Balderas R, Morales-Cruz A, et al: **Phased diploid genome assembly with single-molecule real-time sequencing.** *Nat Methods* 2016, **13**:1050-1054.
17. Gregory TR: **Animal Genome Size Database.** 2017.
18. Parra G, Bradnam K, Korf I: **CEGMA: a pipeline to accurately annotate core genes in eukaryotic genomes.** *Bioinformatics* 2007, **23**:1061-1067.

1
2
3
4
5
6
7
8
9
10
11
12
13
14
15
16
17
18
19
20
21
22
23
24
25
26
27
28
29
30
31
32
33
34
35
36
37
38
39
40
41
42
43
44
45
46
47
48
49
50
51
52
53
54
55
56
57
58
59
60
61
62
63
64
65

19. Parra G, Bradnam K, Ning Z, Keane T, Korf I: **Assessing the gene space in draft genomes.** *Nucleic Acids Res* 2009, **37**:289-297.

20. Zdobnov EM, Tegenfeldt F, Kuznetsov D, Waterhouse RM, Simão FA, Ioannidis P, Seppey M, Loetscher A, Kriventseva EV: **OrthoDB v9.1: cataloging evolutionary and functional annotations for animal, fungal, plant, archaeal, bacterial and viral orthologs.** *Nucleic Acids Res* 2017, **45**:D744-D749.

21. Simão FA, Waterhouse RM, Ioannidis P, Kriventseva EV, Zdobnov EM: **BUSCO: assessing genome assembly and annotation completeness with single-copy orthologs.** *Bioinformatics* 2015, **31**:3210-3212.

22. Zhang G, Li B, Li C, Gilbert MTP, Mello CV, Jarvis ED, Wang J, The Avian Genome C: **Genomic data of the Anna's Hummingbird (*Calypte anna*).** *GigaDB* 2014.

23. Kim D, Pertea G, Trapnell C, Pimentel H, Kelley R, Salzberg SL: **TopHat2: accurate alignment of transcriptomes in the presence of insertions, deletions and gene fusions.** *Genome Biol* 2013, **14**:R36.

24. Jarvis ED, Yu J, Rivas MV, Horita H, Feenders G, Whitney O, Jarvis SC, Jarvis ER, Kubikova L, Puck AEP, et al: **Global View of the Functional Molecular Organization of the Avian Cerebrum: Mirror Images and Functional Columns.** *Journal of Comparative Neurology* 2013, **521**:3614-3665.

25. Whitney O, Pfenning AR, Howard JT, Blatti CA, Liu F, Ward JM, Wang R, Audet JN, Kellis M, Mukherjee S, et al: **Core and region-enriched networks of behaviorally regulated genes and the singing genome.** *Science* 2014, **346**:1256780.

26. Langmead B, Salzberg SL: **Fast gapped-read alignment with Bowtie 2.** *Nat Methods* 2012, **9**:357-359.

27. Shlyueva D, Stampfel G, Stark A: **Transcriptional enhancers: from properties to genome-wide predictions.** *Nat Rev Genet* 2014, **15**:272-286.

28. Veyrac A, Besnard A, Caboche J, Davis S, Laroche S: **The transcription factor Zif268/Egr1, brain plasticity, and memory.** *Prog Mol Biol Transl Sci* 2014, **122**:89-129.

29. Jarvis ED, Nottebohm F: **Motor-driven gene expression.** *Proc Natl Acad Sci U S A* 1997, **94**:4097-4102.

30. Flavell SW, Greenberg ME: **Signaling mechanisms linking neuronal activity to gene expression and plasticity of the nervous system.** *Annu Rev Neurosci* 2008, **31**:563-590.

31. Cortés-Mendoza J, Díaz de León-Guerrero S, Pedraza-Alva G, Pérez-Martínez L: **Shaping synaptic plasticity: the role of activity-mediated epigenetic regulation on gene transcription.** *Int J Dev Neurosci* 2013, **31**:359-369.

32. Stanke M, Diekhans M, Baertsch R, Haussler D: **Using native and syntenically mapped cDNA alignments to improve de novo gene finding.** *Bioinformatics* 2008, **24**:637-644.

33. Liu YX, Wang J, Guo J, Wu J, Lieberman HB, Yin Y: **DUSP1 is controlled by p53 during the cellular response to oxidative stress.** *Mol Cancer Res* 2008, **6**:624-633.

34. Horita H, Wada K, Rivas MV, Hara E, Jarvis ED: **The dusp1 immediate early gene is regulated by natural stimuli predominantly in sensory input neurons.** *J Comp Neurol* 2010, **518**:2873-2901.

35. Fisher SE, Scharff C: **FOXP2 as a molecular window into speech and language.** *Trends Genet* 2009, **25**:166-177.

36. Lai CS, Fisher SE, Hurst JA, Vargha-Khadem F, Monaco AP: **A forkhead-domain gene is mutated in a severe speech and language disorder.** *Nature* 2001, **413**:519-523.

37. Turner SJ, Hildebrand MS, Block S, Damiano J, Fahey M, Reilly S, Bahlo M, Scheffer IE, Morgan AT: **Small intragenic deletion in FOXP2 associated with childhood apraxia of speech and dysarthria.** *Am J Med Genet A* 2013, **161A**:2321-2326.

1
2
3
4
5
6
7
8
9
10
11
12
13
14
15
16
17
18
19
20
21
22
23
24
25
26
27
28
29
30
31
32
33
34
35
36
37
38
39
40
41
42
43
44
45
46
47
48
49
50
51
52
53
54
55
56
57
58
59
60
61
62
63
64
65

38. Haesler S, Wada K, Nshdejan A, Morrisey EE, Lints T, Jarvis ED, Scharff C: **FoxP2 expression in avian vocal learners and non-learners.** *J Neurosci* 2004, **24**:3164-3175.

39. Teramitsu I, White SA: **FoxP2 regulation during undirected singing in adult songbirds.** *J Neurosci* 2006, **26**:7390-7394.

40. Haesler S, Rochefort C, Georgi B, Licznernski P, Osten P, Scharff C: **Incomplete and inaccurate vocal imitation after knockdown of FoxP2 in songbird basal ganglia nucleus Area X.** *PLoS Biol* 2007, **5**:e321.

41. Castellucci GA, McGinley MJ, McCormick DA: **Knockout of Foxp2 disrupts vocal development in mice.** *Sci Rep* 2016, **6**:23305.

42. Chabout J, Sarkar A, Patel SR, Radden T, Dunson DB, Fisher SE, Jarvis ED: **A Foxp2 Mutation Implicated in Human Speech Deficits Alters Sequencing of Ultrasonic Vocalizations in Adult Male Mice.** *Front Behav Neurosci* 2016, **10**:197.

43. Condro MC, White SA: **Recent Advances in the Genetics of Vocal Learning.** *Comp Cogn Behav Rev* 2014, **9**:75-98.

44. Blockus H, Chédotal A: **The multifaceted roles of Slits and Robos in cortical circuits: from proliferation to axon guidance and neurological diseases.** *Curr Opin Neurobiol* 2014, **27**:82-88.

45. Wang R, Chen CC, Hara E, Rivas MV, Roulhac PL, Howard JT, Chakraborty M, Audet JN, Jarvis ED: **Convergent differential regulation of SLIT-ROBO axon guidance genes in the brains of vocal learners.** *J Comp Neurol* 2014.

46. Treangen TJ, Salzberg SL: **Repetitive DNA and next-generation sequencing: computational challenges and solutions.** *Nat Rev Genet* 2011, **13**:36-46.

47. Palazzo AF, Gregory TR: **The case for junk DNA.** *PLoS Genet* 2014, **10**:e1004351.

48. Chin CS, Alexander DH, Marks P, Klammer AA, Drake J, Heiner C, Clum A, Copeland A, Huddleston J, Eichler EE, et al: **Nonhybrid, finished microbial genome assemblies from long-read SMRT sequencing data.** *Nat Methods* 2013, **10**:563-569.

49. She R, Chu JS, Wang K, Pei J, Chen N: **GenBlastA: enabling BLAST to identify homologous gene sequences.** *Genome Res* 2009, **19**:143-149.

50. Slater GS, Birney E: **Automated generation of heuristics for biological sequence comparison.** *BMC Bioinformatics* 2005, **6**:31.

51. Brind'Amour J, Liu S, Hudson M, Chen C, Karimi MM, Lorincz MC: **An ultra-low-input native ChIP-seq protocol for genome-wide profiling of rare cell populations.** *Nat Commun* 2015, **6**:6033.

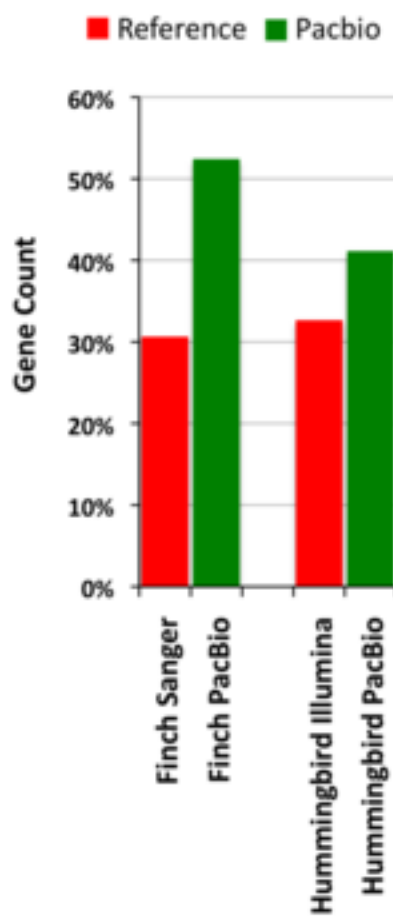
52. Hall TA: **BioEdit: a user-friendly biological sequence alignment editor and analysis program for Windows 95/98/NT.** *Nucl Acids Symp Ser* 1999, **41**:95-98.

53. Krumsiek J, Arnold R, Rattei T: **Gepard: a rapid and sensitive tool for creating dotplots on genome scale.** *Bioinformatics* 2007, **23**:1026-1028.

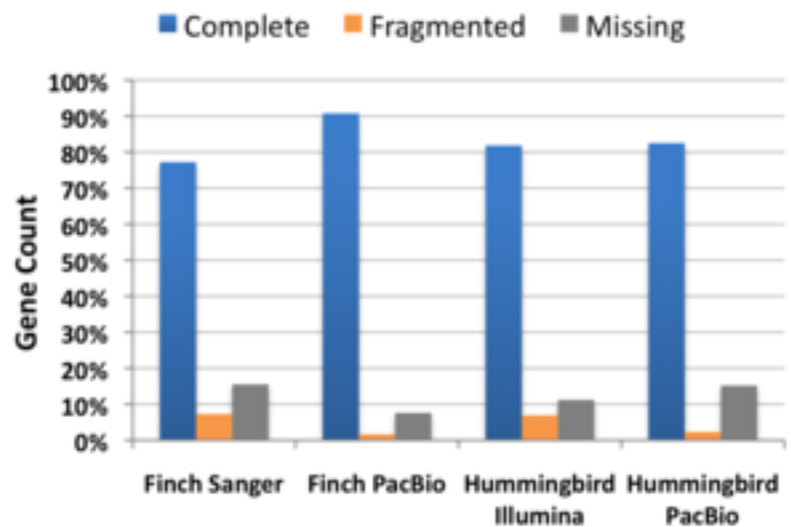
54. Wu TD, Watanabe CK: **GMAP: a genomic mapping and alignment program for mRNA and EST sequences.** *Bioinformatics* 2005, **21**:1859-1875.

55. Chakraborty M, Jarvis ED: **Brain evolution by brain pathway duplication.** *Philosophical Transactions of the Royal Society B-Biological Sciences* 2015, **370**:50056-50056.

A. >95% complete
CEGMA eukaryote
(n=248 genes)



B. BUSCO eukaryote (n=303 genes)



C. BUSCO aves (n=4195 genes)

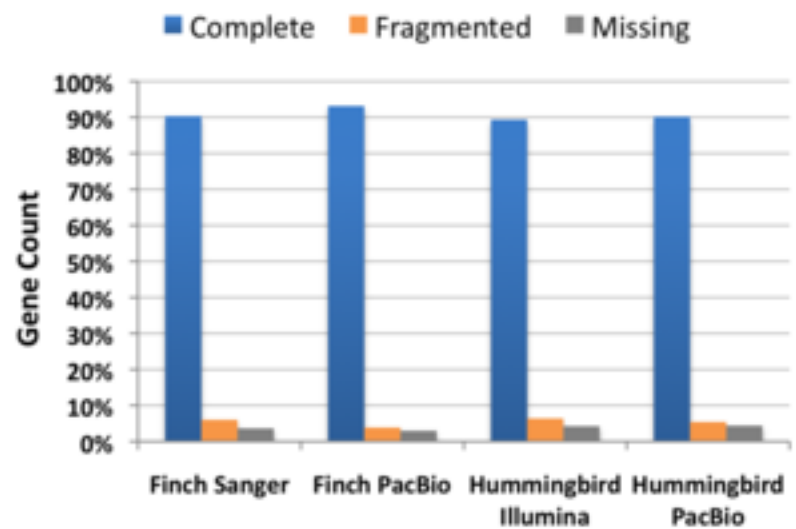
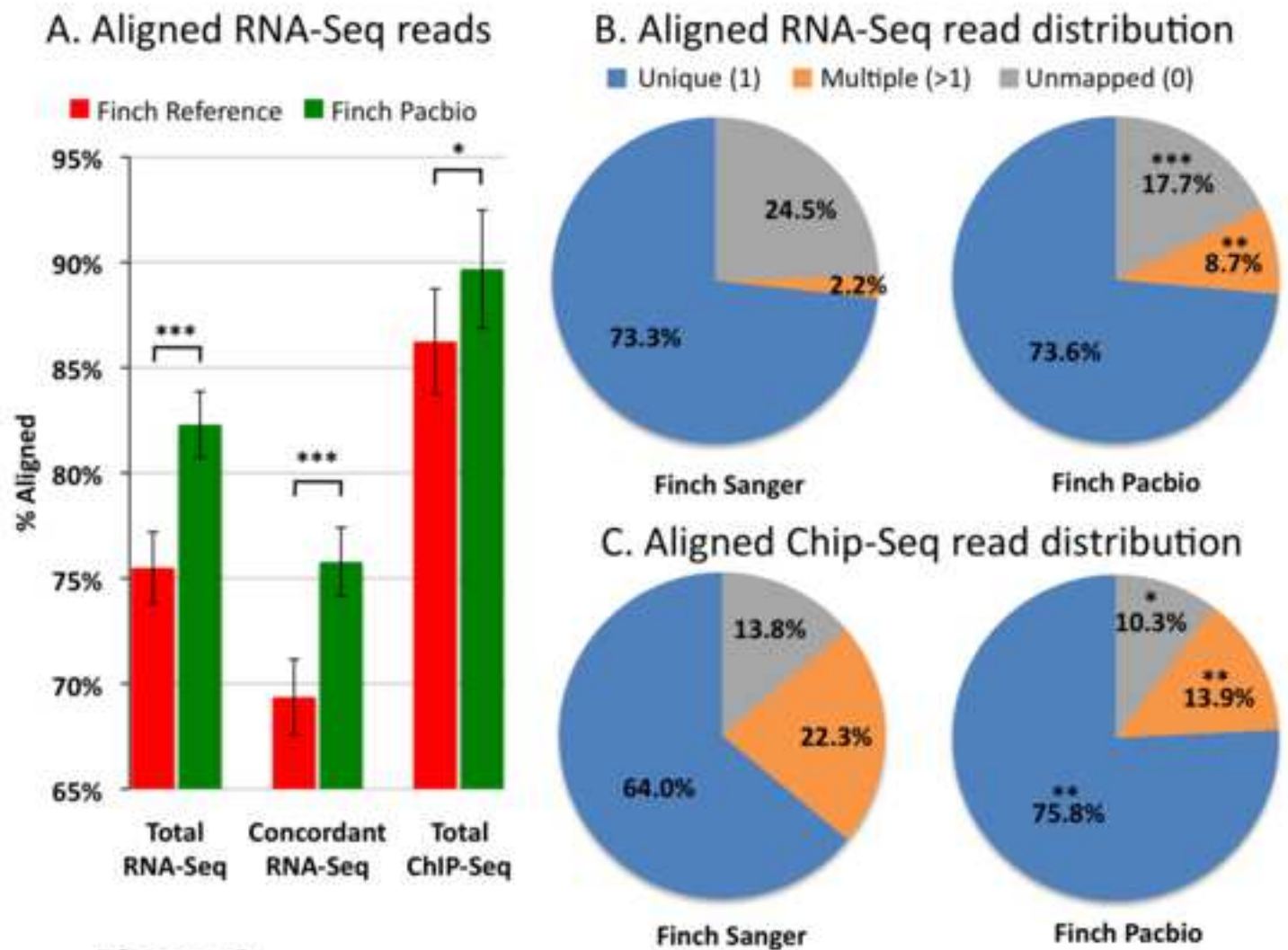


Figure 1

**Figure 2**

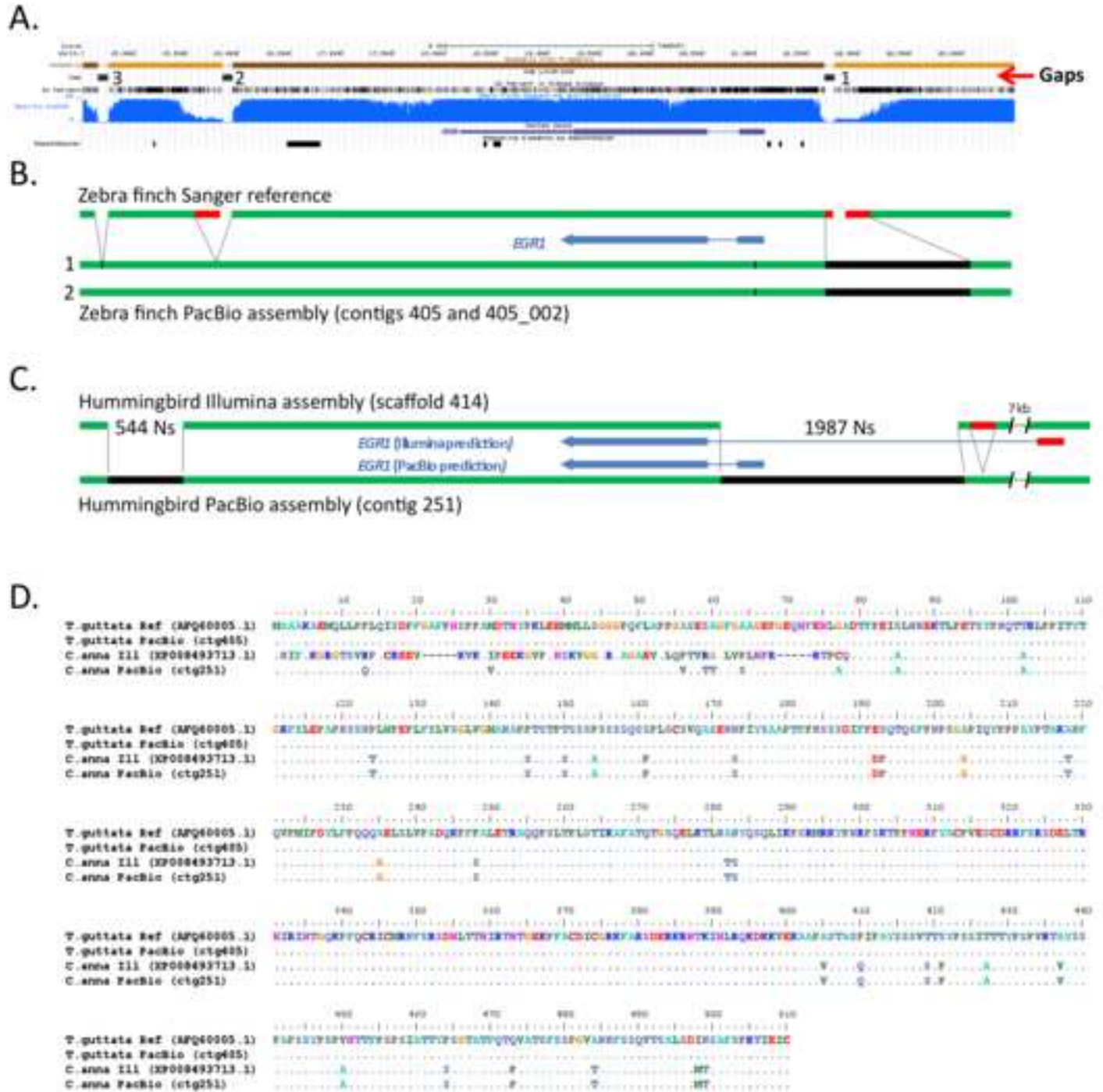


Figure 3



Figure 4

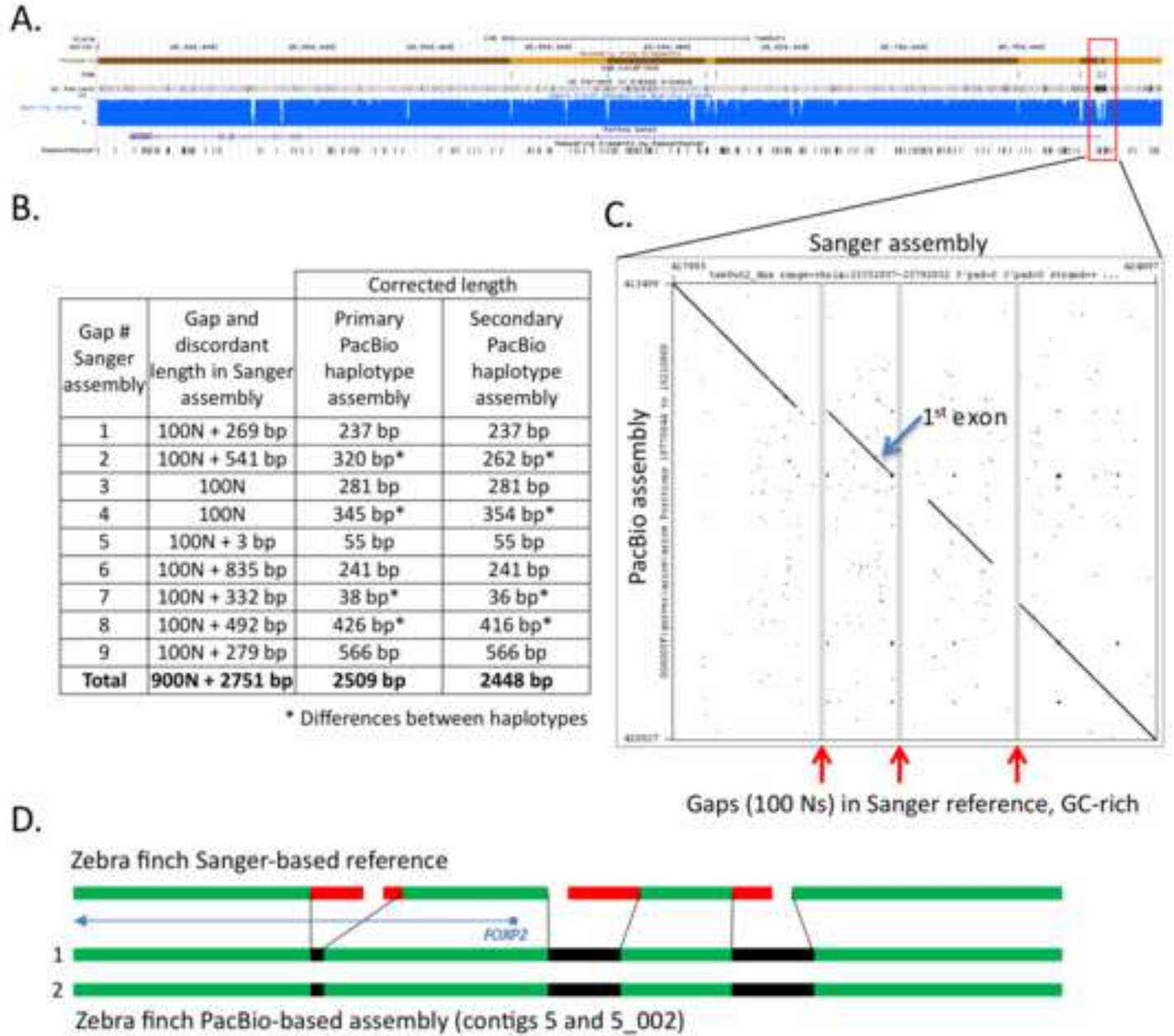


Figure 5



[Click here to access/download](#)

Supplementary Material

Korlach et al supplementary figures.pdf

